



KARL-FRANZENS-UNIVERSITÄT GRAZ

Masses of custodial singlet vector particles in Yang-Mills-Higgs theory

MASTERARBEIT

zur Erlangung des akademischen Grades MSc
am Institut für Physik
der Karl-Franzens-Universität Graz

vorgelegt von:
Dominik Nitz

Betreuer:
Prof. Axel Maas

Graz, Februar 2019

Abstract

The correlation functions and effective masses of three operators were calculated for the Yang-Mills-Higgs theory, i.e. an $SU(2)$ gauge theory with a complex scalar doublet. The operators we used are custodial singlet vectors only containing gauge fields, i.e. so-called W-balls. The lattices these objects were studied on are hypercubic and of size 8^4 , 12^4 and 16^4 . Smearing was implemented to handle statistical noise. The operators we used do not show significant overlap with low-mass states. The lowest state is far above the lattice cut-off and the mass of a scattering state of two Higgs bosons.

Kurzfassung

Die Korrelationsfunktionen und effektiven Massen von drei Operatoren wurden in der Yang-Mills-Higgs-Theorie, d.h. $SU(2)$ -Eichtheorie mit einem komplexem skalaren Dublett, berechnet. Die verwendeten Operatoren sind Singulets in der custodialen Gruppe und Vektoren. Sie sind W-Bälle, das heißt sie bestehen ausschließlich aus Eichfeldern. Die verwendeten Gitter sind hyperkubisch und haben die Größen 8^4 , 12^4 und 16^4 . Smearing wurde implementiert um das statistische Rauschen zu dämpfen. Die Operatoren zeigen keinen signifikanten Überlapp mit Zuständen niedriger Masse und sogar der niedrigste Zustand liegt weit über dem Gitter-Cutoff und hat eine weit höhere Masse als der Streuzustand zweier Higgsbosonen.

Contents

1	Introduction	3
2	$SU(2)$-Yang-Mills-Higgs theory	5
2.1	Gauge Theories	5
2.2	Yang-Mills-Higgs theory	5
2.3	Perturbation theory	7
2.4	Channels, quantum numbers and spin	8
2.5	Choice of operators	9
2.6	The operators	10
3	Lattice field theory	12
3.1	Lagrangian	12
3.2	Configurations	12
3.3	Mass spectroscopy	13
3.4	Smearing	14
4	Implementation	15
4.1	Operator implementation	15
4.2	Computation time	15
5	Results	16
5.1	Parameter set 1	16
5.2	Parameter set 2	20
6	Conclusion	22
7	Appendix - Wilson loop implementation	23

1 Introduction

The Standard Model of particle physics [1] is a collection of theories that together comprise our best attempt at describing the dynamics of elementary particles. It is well backed by experiments and describes all observed phenomena very well. Nevertheless, it is not perfect. It does not contain a description of quantum gravity and is not valid for arbitrarily high energies. One part of the Standard Model is a Yang-Mills-Higgs theory, the topic of this thesis. It describes weak interactions and today it is easily accessible by lattice computations.

The weak interaction is, like quantum electrodynamics (QED) and quantum chromodynamics (QCD), a gauge theory. That is a theory which has as its base a gauge symmetry and a corresponding gauge group. It is very curious that a simple gauge invariance can give rise to a quantum field theory that describes reality. A common few is that gauge invariance is thus an important fundamental aspect of our world. In contrast, some see gauge invariance just as the veneer of a deeper principle of the universe. In my opinion this situation bears resemblance to Plato's cave.

The weak interaction is an experimentally well backed and mature theory. Still, there are some topics for which there is no consensus in the physics community. One of these is the question of gauge invariance in regard to observable field operators. That any sensible observable must be gauge invariant needs not to be said. Still, perturbation theory of some non-gauge invariant operators yields good results that agree with experiments. To tackle this problem, a gauge invariant perturbation theory has been proposed [2, 3], and already some studies to confirm it, have been done [4, 5, 6]. Because non-gauge invariant perturbation theory works so well in the context of the Standard Model, the theory has not yet gained wide awareness.

Investigations into the Standard Model on the lattice are always restricted to the subsectors of the full model. The use of simpler gauge groups and the omission of fermions in favour of bosons are practices to avoid the large effort, needed to implement them, but still retain the interesting physics.

In this research we aim to add one small piece to the puzzle that is the theory of the weak interaction by examining a small number of operators of one channel in a simplified version of the theory. This examination could find problems with the perturbative approaches currently used, or even find hints of a new particle to be discovered in the current model of the weak interaction.

This thesis gives a short introduction into $SU(2)$ -Yang-Mills-Higgs theory and investigates its behaviour by calculating correlation functions and effective masses for a set of operators on the lattice. Chapter 2 gives an introduction into gauge theories and defines the Yang-Mills-Higgs theory. Some of its properties are discussed and the gauge invariant operator we used in the calculations are also addressed. In Chapter 3 some methods necessary for lattice calculations, namely configuration generation, mass spectroscopy, time slice averaging, transformation into the rest frame and smearing are explained. Chapter 4 shows how some of these methods were implemented, and Chapter 5 contains the results obtained from the calculations. Lastly, in Chapter 6 the conclusion of this research is drawn, and the Appendix 7 shows an interesting excerpt of the code used for the computations.

2 $SU(2)$ -Yang-Mills-Higgs theory

This chapter gives an introduction into the definition and properties of a $SU(2)$ gauge theory with a scalar field in the fundamental representation of the gauge group. This theory is easy to implement, but still close enough to the Standard Model to give related results. We start by introducing the concept of gauge theories in general and Yang-Mills-Higgs theory specifically. Gauge invariant perturbation theory is discussed and contrasted with the standard perturbative approach. These approaches are important to understand the recent research into this subject and objectives of this thesis.

2.1 Gauge Theories

QED was one of the first quantum field theories to be devised, and thus in the progress of its development physicists learned a lot about the structure of quantum field theories. Many important properties of the theory were found to be a consequence of gauge invariance. The QED Lagrangian is invariant under an $U(1)$ gauge transformation and very central properties of the theory, like the conservation of current and thereby the Ward identity, follow from this local symmetry. Postulating $U(1)$ gauge invariance and some other restrictions, one can directly derive the QED-Lagrangian, as is done in [7]. This derivation can be generalized to other more complicated groups, which gives rise to a vast number of possibilities for different quantum field theories. The choice of a particular gauge group alone leads to a Lagrangian with only a handful of terms, which may be suitable to form a quantum field theory. The first theory of this kind was found by Yang and Mills [8] and is now known as Yang-Mills-theory.

2.2 Yang-Mills-Higgs theory

Yang-Mills-Higgs theory is one of the most studied examples of a non-abelian gauge theory. It is obtained using $SU(2)$ as gauge group, $SU(2)$ as the custodial group and a complex scalar doublet in the fundamental representation of the gauge group. This theory is part of the Standard Model of particle physics in the so-called Higgs-sector. Yang-Mills-Higgs theory can be compared to experiments to a certain extent, though without the rest of the Standard Model (QED, fermions etc.) certain differences occur. One consequence for example is that the W and Z -bosons are mass-degenerate in this theory.

To introduce the nomenclature, which is a mix of the one in [7] and [9], here follows a short version of the derivation of the theory from the principle of $SU(2)$ gauge invariance. We start by postulation a complex doublet of scalar fields with some potential $V(\phi)$,

$$\mathcal{L} = (\partial_\mu \phi^\dagger)(\partial^\mu \phi) - V(\phi) \tag{1}$$

and a local transformation of these fields

$$\phi(x) \rightarrow \exp\left(i\alpha_i(x)\frac{\sigma^i}{2}\right)\phi(x), \quad (2)$$

where σ^i are the Pauli matrices and $\alpha(x)$ are local coefficients, meaning that they are arbitrary functions of x . This transformation is then different for every point in space, which makes keeping the Lagrangian gauge-invariant more intricate than in the global case. To keep the kinetic term of the scalar fields gauge-invariant the covariant derivative D_μ , containing the gauge fields W_μ^a , has to be introduced:

$$D_\mu = \partial_\mu - igW_\mu^i\frac{\sigma^i}{2} \quad (3)$$

The gauge field's kinetic term uses the field strength tensor $F_{\mu\nu}^i$

$$F_{\mu\nu}^i = \partial_\mu W_\nu^i - \partial_\nu W_\mu^i + g\epsilon^{ijk}W_\mu^jW_\nu^k \quad (4)$$

with the structure constants of the fundamental representation of SU(2) ϵ^{ijk} . With these definitions the gauge invariant Lagrangian is given by

$$\mathcal{L} = -\frac{1}{4}(F_{\mu\nu}^i)^2 + (D_\mu\phi)^\dagger(D^\mu\phi) - V(\phi), \quad (5)$$

which superficially looks like the scalar QED Lagrangian but has a more complicated structure hidden beneath a familiar notation. The custodial group, we mentioned above is a global symmetry of the Lagrangian. This can be explained in the following way: The complex scalar doublet has four degrees of freedom. The free scalar theory thus exhibits a $O(4)$ -symmetry. This is isomorphic to $SU(2) \times SU(2)$ and using one as the gauge group the second remains. The custodial triplet 1_3^- for example is equivalent to the three observed W- and Z-bosons.

Properties

The 0_1^+ and 1_3^- channels are the most interesting, because their ground states are usually identified as the physical Higgs boson and W-bosons respectively. The notation and its meaning is explained in Section 2.4.

Phase diagram: Yang-Mills-Higgs theory shows widely varying behaviour over its phase space. In fact, there exist two distinct regions in the phase diagram [10]. In QCD the non-abelian gauge group is associated with confinement and truly, the first region is a QCD-like region where QCD-like bound states including confinement [11], but no Brout-Englert-Higgs (from now on BEH) effect was observed. In the QCD-like region

the lightest state in the spectrum is in the 0_1^+ -channel [12]. The other region is the BEH-like region where in appropriate gauges a non-vanishing vacuum expectation value for the scalar field is observed. In the BEH-like region the 1_3^- channel contains the ground state [12]. For our work we are interested in the BEH-like region, because there a non-gauge invariant perturbative approach is possible [2, 5, 6]. Fradkin and Shenker found that for the case of $SU(2)$ as the gauge group and the scalar fields in the fundamental representation the QCD-like and the BEH-like phase are smoothly connected [13]. That means there is no phase transition separating them and the two phases thus show only quantitative, not qualitative differences. Thus states found in our calculations should be present at other phase space points as well.

Mass spectrum: Early calculations determining the phase diagram were, for example, done by Lang et al. in the 1980s [14]. In one study Maas and Mufti looked at the lowest masses in the scalar singlet channel, using lattice calculations for a wide range of phase space points [10]. In another they looked very thoroughly at the spectrum in large parts of the phase space, also giving a detailed introduction into the topic of spectroscopy [15]. Wurtz and Lewis determined the mass spectrum of all lattice spin channels for one specific parameter set in the BEH-like region [16]. At some points in the phase diagram there is, like in the Higgs sector, just a Higgs-like and a W-boson-like state. At other points however, there are additional states, e.g. in the 0_1^- channel that if found would represent new physics [15]. One of the goals of this thesis is to expand the knowledge of this spectrum.

2.3 Perturbation theory

In most particle physics textbooks the standard perturbative approach is given. In contrast to this approach a new gauge invariant way of doing perturbation theory has been developed. This approach, though being more rigorous, has not yet found wide attention. The reason for this is the fact that for the Standard model standard perturbation theory is equivalent to gauge invariant perturbation theory.

To do perturbation theory the following steps are made. The potential $V(\phi)$ is usually chosen to have the form of a Mexican hat $V(\phi) = (\phi^\dagger\phi - f^2)^2$. This potential is minimal when $\phi^\dagger\phi = f^2$ and shows a symmetry under the gauge group and custodial group. Using this minimum the scalar field can be split into two parts.

$$\phi(x) = \frac{v}{\sqrt{2}}n + \varphi(x) \tag{6}$$

Here v is a constant, n is a unit vector in some direction. Together they point to a minimum of the potential and φ is a fluctuation field around this minimum $\langle\varphi\rangle = 0$. This split hides the gauge symmetry.

Standard perturbation theory Perturbation theory requires the scalar field to have a non-vanishing expectation value. Due to the gauge symmetry of the potential this not the case. When taking the path integral all minima are integrated over and the expectation value becomes zero. The solution is to fix the gauge and thereby choose a minimum. One common method is the Faddeev-Popov method [7]. This gauge fixing explicitly breaks the gauge symmetry. Continuing this approach yields a Lagrangian containing gauge fixing terms and ghost terms and it yields three equally massive gauge bosons and a massive scalar Higgs-field. In the 1_1^- -channel standard perturbation shows no particles, thus finding a state in lattice calculations would stand in conflict with this approach.

Gauge invariant perturbation theory The standard perturbation theory thus agrees with experiments, but there is a problem. Of course observables need to be gauge invariant to be physically meaningful. But because standard perturbation theory in the Higgs sector works very well, the fact that the elementary operators are not gauge invariant is often ignored. This disconnect between phenomenologically confirmed perturbation theory and theoretically motivated rigorous quantum field theory even resulted in the different uses of the name Higgs particle. Whereas in perturbation theory the scalar field $\phi(x)$ itself is often referred to as Higgs, in the lattice-QFT community this term is mostly used for describing the composite operator $\phi(x)^\dagger\phi(x)$.

The reason that these two very different approaches both lead to similar results is a peculiarity of $SU(2)$. In [2, 3] a gauge invariant perturbation theory (GIPT) is proposed, which shows that under certain conditions, fulfilled by the Standard Model, the physical states can be mapped to the gauge-dependend states in the Lagrangian. Using GIPT one can show that some of the composite operators yield the same mass as the elementary field operators to leading order. And thus GIPT is an attempt to bring the phenomenology together with rigorous quantum field theory. Calculations have been done that confirm this theory in [4, 5, 6].

The insight that these specific conditions have to be met by the Standard Model excludes some proposals for extensions to the Standard Model. This fact will be useful in identifying suitable new theories and in this thesis we also try to contribute a small part to this. The low-lying particle spectrum of beyond-Standard Model theories could show differences to the current Standard Model and in our work we aim to find such low-lying states in the 1_1^- -channel, introduced in the next section.

2.4 Channels, quantum numbers and spin

In the last section we saw that because of gauge invariance composite operators have to be used in lattice field theory calculations. This section gives an overview of the characterisation of these operators.

Table 1: The number of copies of each cubic lattice representation Λ of the group of rotations for continuum spins J

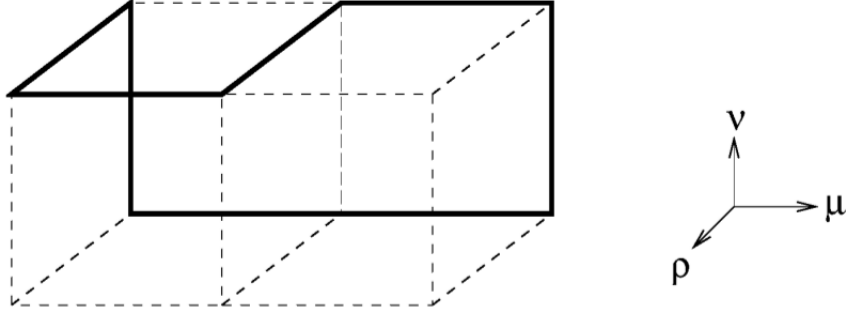
$\Lambda \backslash J$	0	1	2	3	4
A_1	1	0	0	0	1
A_2	0	0	0	1	0
E	0	0	1	0	1
T_1	0	1	0	1	1
T_2	0	0	1	1	1

Quantum mechanics states that only states with equal quantum numbers mix. Thus the operators used can be put into categories called channels, described by notation introduced below. The three operators that will be used here are custodial singlet vector operators. The reasons we chose this channel are discussed in Section 2.5. In the continuum notation the operators are denoted as $J_c^P = 1_1^-$. J is the total angular momentum, P is the parity quantum number and c is the custodial quantum number. Because $SU(2)$ is a pseudo-real group, the charge conjugated states are equivalent and there is no need for the charge conjugation quantum number C . The total angular momentum is made up from the angular momenta of the constituents and a possible relative angular momentum between them. This relative momentum is important in the interpretation of states in the mass spectrum.

There is one more complication. On a cubic lattice, the spin representations differ from the ones in the continuum [17]. In the continuum limit the lattice representations transform into the continuum representations according to Table 1. Unfortunately the transformation is not always one-to-one, but from Table 1 we see that only the lattice spin representation T_1 corresponds to the spin $J = 1$ in the continuum. This representation is the vector representation. More on this topic in the context of lattice simulations can be found in [17].

2.5 Choice of operators

The motivation for using operators of the 1_1^- channel is twofold. The first reason is to try to falsify GIPT and standard perturbation theory. Neither predicts elementary particles in this channel. Thus finding such a state would disprove these theories. The second motive was to find a sign of a Z' boson. There is ongoing research into finding experimental signs of this hypothetical particle, e.g. [18]. If it exists it is expected to be found using today's collider experiments, but to date it has not been found. Were a state in the 1_1^- -channel to be detected on the lattice, it would show that a potential 'new physics-discovery' of the Z' boson was not new physics but just an effect of the Standard Model. The construction of the operators we used for the calculations is described in the next section.

Figure 1: The Wilson loop operator $W_{\mu\nu\rho}$. [16]

2.6 The operators

Simple and basic operators for the theory can be found in [15], and a complete set of operators for all available angular momentum and parity quantum numbers can be found in [16]. The latter paper is also the source for the operators that were used in the computations here. Only W-Ball operators from the T_1 -channel were used. W-Balls, like glueballs (their QCD-equivalents), are operators which are exclusively built from gauge field operators. More on the reasons for choosing these operators can be found in the last section.

All operators here are built from linear combinations of a single operator, namely the Wilson loop operator

$$W_{\mu\nu\rho}(t) = \frac{1}{2} \text{Tr} \sum_{\vec{x}} U_{\mu}(x) U_{\mu}(x + \hat{\mu}) U_{\nu}(x + 2\hat{\mu}) U_{\mu}^{\dagger}(x + \hat{\mu} + \hat{\nu}) \times U_{\rho}(x + \hat{\mu} + \hat{\nu}) U_{\mu}^{\dagger}(x + \hat{\nu} + \hat{\rho}) U_{\rho}^{\dagger}(x + \hat{\nu}) U_{\nu}^{\dagger}(x), \quad (7)$$

shown in Fig. 1. The operators are rather complex, thus these linear combinations are introduced.

$$B_{\mu\nu\rho}^{-} = + W_{+\mu+\nu+\rho} + W_{+\mu+\nu-\rho} + W_{+\mu-\nu+\rho} + W_{+\mu-\nu-\rho} - W_{-\mu+\nu+\rho} - W_{-\mu+\nu-\rho} - W_{-\mu-\nu+\rho} - W_{-\mu-\nu-\rho} \quad (8)$$

$$C_{\mu\nu\rho}^{-} = + W_{+\mu+\nu+\rho} + W_{+\mu+\nu-\rho} - W_{+\mu-\nu+\rho} - W_{+\mu-\nu-\rho} + W_{-\mu+\nu+\rho} + W_{-\mu+\nu-\rho} - W_{-\mu-\nu+\rho} - W_{-\mu-\nu-\rho} \quad (9)$$

$$D_{\mu\nu\rho}^{-} = + W_{+\mu+\nu+\rho} - W_{+\mu+\nu-\rho} + W_{+\mu-\nu+\rho} - W_{+\mu-\nu-\rho} + W_{-\mu+\nu+\rho} - W_{-\mu+\nu-\rho} + W_{-\mu-\nu+\rho} - W_{-\mu-\nu-\rho} \quad (10)$$

They are odd under parity, indicated by the - index, and used to build the following custodial singlet operators.

$$\mathcal{O}_1 = \begin{pmatrix} B_{123}^- + B_{132}^- \\ B_{231}^- + B_{213}^- \\ B_{312}^- + B_{321}^- \end{pmatrix} \quad (11)$$

$$\mathcal{O}_2 = \begin{pmatrix} C_{123}^- + C_{321}^- \\ C_{231}^- + C_{132}^- \\ C_{312}^- + C_{213}^- \end{pmatrix} \quad (12)$$

$$\mathcal{O}_3 = \begin{pmatrix} D_{123}^- + D_{213}^- \\ D_{231}^- + D_{321}^- \\ D_{312}^- + D_{132}^- \end{pmatrix} \quad (13)$$

These operators transform under the T_1 representation and are therefore vectors. This fact is going to be useful to check the correctness of the implementation, as is discussed in Chapter 4.

3 Lattice field theory

In the last chapter we introduced the theory and the composite operators we want to examine. In this chapter we discuss the methods we used to compute their masses. Lattice field theory is a non-perturbative approach, well suitable for the calculation of the bound states masses. We start by introducing the Lagrangian and the configuration generation we used. The calculation of correlation functions on the lattice is then explained together with smearing, a method to deal with the statistical noise of the measurements.

3.1 Lagrangian

The lattice action used [15, 19] is

$$S = \beta \sum_x \left(1 - \frac{1}{2} \sum_{\mu < \nu} \Re \text{Tr} U_{\mu\nu}(x) \right) + \sum_{\vec{x}} \left(\phi^\dagger(x) \phi(x) + \lambda (\phi(x)^\dagger \phi(x) - 1)^2 - \kappa \sum_{\mu} (\phi(x)^\dagger U_{\mu}(x) \phi(x + e_{\mu}) + \phi(x + e_{\mu})^\dagger U_{\mu}(x)^\dagger \phi(x)) \right) \quad (14)$$

with

$$U_{\mu\nu}(x) = U_{\mu}(x) U_{\nu}(x + e_{\mu}) U_{\mu}(x + e_{\nu})^\dagger U_{\nu}(x)^\dagger \quad (15)$$

$$W_{\mu} = \frac{1}{2agi} (U_{\mu}(x) - U_{\mu}(x)^\dagger) + \mathcal{O}(a^2) \quad (16)$$

$$\beta = \frac{4}{g^2} \quad (17)$$

$$a^2 m_0^2 = \frac{(1 - 2\lambda)}{\kappa} - 8 \quad (18)$$

$$\lambda = \kappa^2 \gamma. \quad (19)$$

Here a is the lattice spacing, U_{μ} the gauge-link $\exp(igaW_{\mu})$, e_{μ} the unit vector in the μ -direction and β, κ, λ are the lattice coupling parameters.

3.2 Configurations

The configuration generation follows [6] and was indeed done using the same code. Before measuring starts, there is a phase for the system to reach equilibrium, which consists of 4096 sweeps. In a sweep the gauge fields are updated using a heat-bath sweep, and a Metropolis sweep is used for the Higgs field. 24 such sweeps are done between every measurement. The error calculation has been done by the statistical bootstrap method. 1000 resamplings were done, and the 67% interval of these errors was taken.

3.3 Mass spectroscopy

This section gives an overview of the procedure to obtain the masses of the operators from Section 2.6. This is the central technical subject of this thesis. The quantities measured on the lattice are the operator values at each space-time point. These operators are then combined to form the correlators $C(\Delta t)$ as follows.

$$C(\Delta t) = \langle \mathcal{O}(t)\mathcal{O}(t + \Delta t) \rangle \quad (20)$$

The product $\mathcal{O}(t)\mathcal{O}(t + \Delta t)$ is a scalar product over the vector components. And the expectation value is achieved by a sum over the configurations. Because of time invariance an average of the correlator at different times is taken. This procedure is called time slice averaging. The operator is added up at all space points, which is equivalent to a Fourier transformation with zero momentum. Thus this gives the correlation function for zero relative momentum, i.e. the rest frame.

$$\mathcal{O}(\Delta t) = \sum_{\vec{x}} \mathcal{O}(\vec{x}, \Delta t) \quad (21)$$

The result is a function only of Δt . This correlator is used to determine the mass of the states. If we take $|n\rangle$ to be a set of states in the spectrum with corresponding energy E_n ($E_n \leq E_{n+1}$) the function can be expressed as a sum over exponentials multiplied by an overlap.

$$C(\Delta t) = \langle \mathcal{O}(\Delta t)\mathcal{O}(0) \rangle = \sum_n |\langle n|\mathcal{O} \rangle|^2 \exp(-E_n \Delta t) \stackrel{\Delta t \gg E_1^{-1}}{\sim} \text{const.} \cdot \exp(-E_0 \Delta t) \quad (22)$$

Because of the projection to zero momentum in equation (21), the energy E_n directly corresponds to the mass. It is easy to see that the exponential term for the ground state falls the slowest, thus for large Δt we can extract the mass by a fit. All of this relies on the fact that there is a large enough overlap between the chosen operator and the ground state. To extract higher state masses, one can do a variational analysis on the correlation matrix that consists of correlators of a set of operators. This will not be done here.

An important quantity is the effective mass $m_{eff}(\Delta t)$,

$$m_{eff}(\Delta t) = \ln \frac{C(\Delta t)}{C(\Delta t + 1)}, \quad (23)$$

which for a dominating ground state approximates the ground state mass. For small Δt the error is larger because of contributions from higher states, which results in a higher effective mass.

3.4 Smearing

Noise reduction is a significant problem when doing mass spectroscopy. Therefore, a technique called smearing is introduced. A link connecting two neighbouring points is replaced by a sum over link combinations that connect the same points. This average over different paths reduces noise, but also quenches the information of the operator. Smearing can be done multiple times and operators measured after each of these smearing steps are independent from each other. Thus a set of operators used for variational analysis can contain 'the same operator' but evaluated at different smearing steps. When deciding how many smearing steps are to be used, one has to strike a balance between keeping enough signal of the operators and reducing noise. A rule of thumb is that the maximum number of smearing steps should be $\leq N$, because beyond that smearing will wrap-around and mix any link, going through the periodic boundary conditions, with itself. There are different smearing schemes, though the one used in this thesis is called APE smearing [20, 21]:

$$U_\mu^{(n)}(x) = \frac{1}{\sqrt{\det R_\mu^{(n)}(x)}} R_\mu^{(n)}(x) \quad (24)$$

$$\begin{aligned} R_\mu^{(n)}(x) &= \alpha U_\mu^{(n-1)}(x) + \frac{1-\alpha}{2(d-1)} \\ &\times \sum_{\nu \neq \mu} (U_\nu^{(n-1)}(x+e_\mu) U_\mu^{(n-1)\dagger}(x+e_\nu) U_\nu^{(n-1)\dagger}(x) \\ &+ U_\nu^{(n-1)\dagger}(x+e_\mu-e_\nu) U_\mu^{(n-1)\dagger}(x-e_\nu) U_\nu^{(n-1)}(x-e_\nu)) \end{aligned} \quad (25)$$

$$\begin{aligned} \phi^{(n)}(x) &= \frac{1}{1+2(d-1)} (\phi^{(n-1)}(x) \\ &+ \sum_{\mu} (U_\mu^{(n-1)}(x) \phi^{(n-1)}(x+e_\mu) + U_\mu^{(n-1)}(x-e_\mu) \phi^{(n-1)}(x-e_\mu))) \end{aligned} \quad (26)$$

with $\alpha = 0.55$ and $d = 4$.

4 Implementation

This short chapter gives some information about how we implemented the methods of Chapter 3. The program for the configuration generation was written by Axel Maas in C++, and for validation some measurements were compared to earlier studies. The measurement routine for this thesis was implemented in a header file for that program.

4.1 Operator implementation

The operators were introduced in Section 2.6. The linear combinations of equations (8-10) were implemented using the `#define` directive. This is just a matter of correctly copying the signs of the directional indices. To implement the Wilson loop operator in equation (7) is of more difficult. The indices in $W_{\mu\nu\rho}$ designate the orientation of the operator in space. The challenge is to assign to each link in the Wilson loop operator the correct spatial dependencies, so as to create a continuous path in space. This is achieved by a function shown in Appendix 7. This function was tested by manually implementing the function for every direction separately and comparing the results. Another procedure that was implemented to test the correctness of the implementation was a set of lattice reflection functions. Because all implemented operators are vectors, they exhibit a simple sign changing behavior under these transformations, which acts as a hint that the implementation is correct.

4.2 Computation time

The computation time used to obtain the results of this thesis was approximately 106000 core hours (4400 core days) on HPC cluster computers of the University of Graz.

5 Results

In this chapter we present the results of the mass measurements of the gauge invariant operators from Section 2.6 using the methods introduced in Chapter 3. We used two different parameter sets, which were chosen for their physical mass ratio $m_{1_3^-}/m_{0_1^+}$. The coupling for both sets is larger than the physical one, but this should not qualitatively change the results of this thesis. The reason not to choose a parameter set where the coupling corresponds to the physical one is that the theory is fine-tuned and such a parameter set has not yet been found.

The lattices used were 4-dimensional hypercubes with sides $N = 8, 12, 16$. We computed 957000 configurations for each lattice size. Measurements were done after 0, 1, 4, 8 and 16 smearing steps. The errors were calculated using a 67% confidence interval of the statistical bootstrap method and results which are compatible with zero within the determined error are omitted in the plots. The three different operators we used, gave qualitatively the same results, and therefore only the results of one of these operators, namely \mathcal{O}_2 from equation (12), are presented here.

5.1 Parameter set 1

The parameters for the first set of calculations are $\beta = 2.7984$, $\kappa = 0.2927$ and $\lambda = 1.317$. At this phase space point the lattice spacing is $a^{-1} = 453\text{GeV}$, the coupling is $\alpha_{200\text{GeV}} = 0.605$ and the mass ratio is $m_{1_3^-}/m_{0_1^+} = 80\text{GeV}/124(3)\text{GeV}$. All errors are $< 1\%$, except when specified otherwise. This parameter set lies within the BEH-like region, which makes the approach using GIPT possible. In the following plots all quantities are given in lattice units.

Technical details

To examine the technical details of the measurements, some plots of correlators will be presented. First, the effect of smearing, as outlined in Section 3.4, will be looked at. Therefore in Figure 2 the correlators with error bands for $N = 8$ are shown. Smearing dampens the statistical noise and we can see that for the amount of measurements taken, only the 16 times smeared operator shows proper behaviour for all 5 time steps. Even though 16 smearing steps will dampen the signal of potentially interesting states strongly, this correlator is studied in more detail. We are interested in low mass states, therefore the suppression of higher states should not be a problem. On the $N = 16$ lattice, a wrap-around effect due to smearing does not occur. To study finite volume effects, in Figure 3 the correlators for $N = 8, 12, 16$ are compared at smearing step 16. The statistical noise was so substantial, that for lattice sizes $N = 12, 16$ only the first 5 measurements were

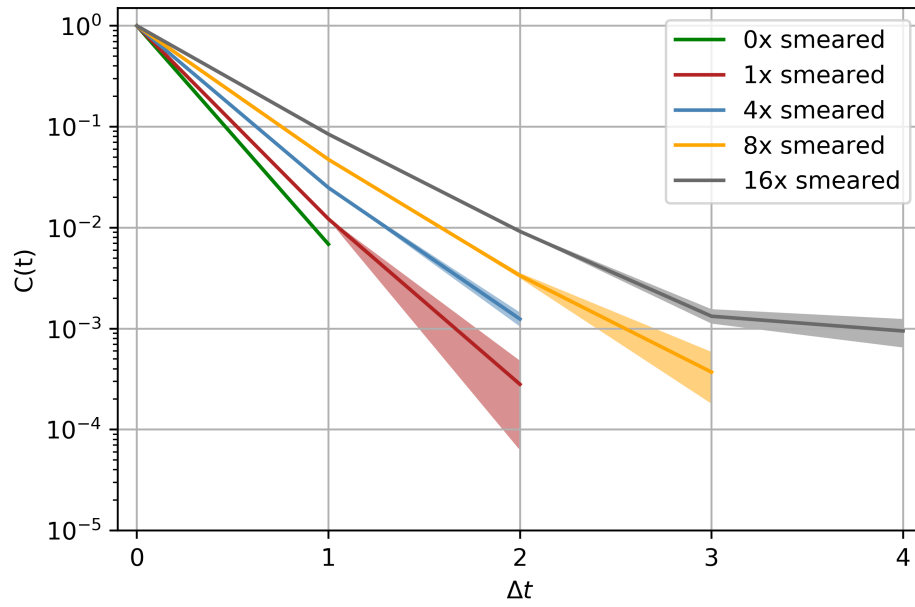
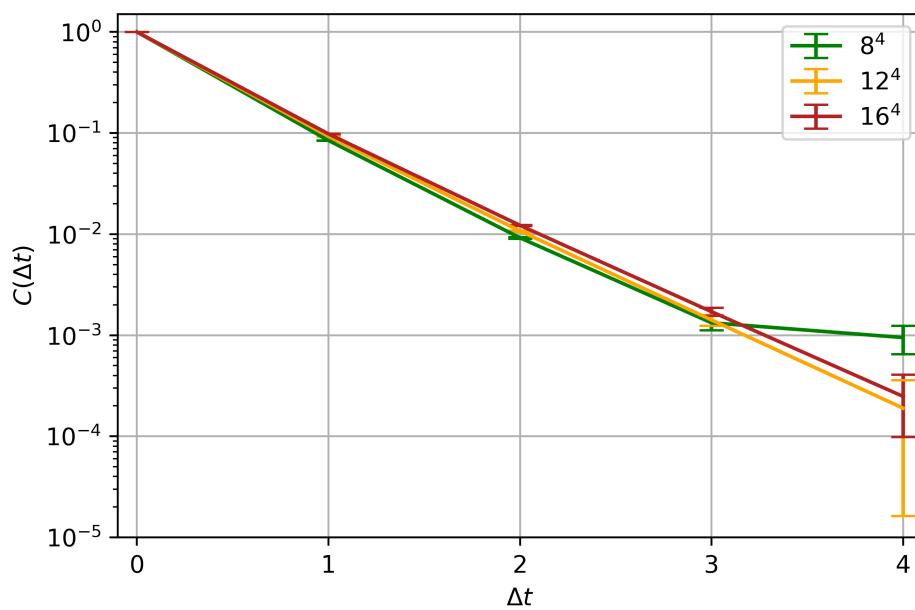
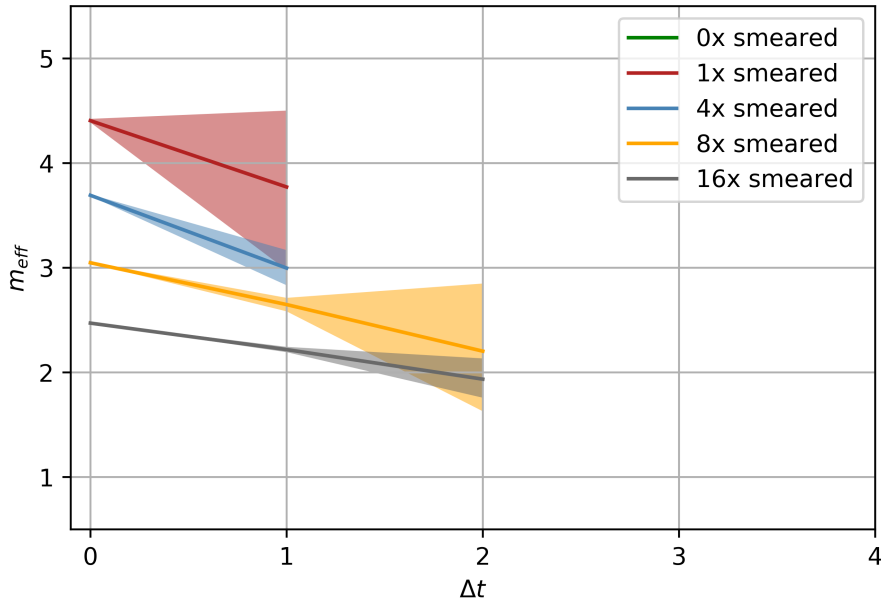
Figure 2: The correlators for parameter set 1 and $N = 8$ at different smearing levels.Figure 3: The correlators for parameter set 1 and $N = 8, 12, 16$ at smearing level 16.

Figure 4: The effective masses for parameter set 1 and $N = 8$ at different smearing levels.

statistically significant. From the data that was usable one can see that the correlators' dependence on volume is very small.

Effective mass

The physically relevant quantity is the effective mass, as defined in equation (23), and it will be examined now. In Figure 4-6 the effective masses for $N = 8, 12, 16$ are shown.

This shows that the effective mass of the lowest measured state lies approximately at $am \approx 2$, which corresponds to 906GeV. This high mass lies above the lattice cut-off and the mass of a combination of two 0_1^+ ground states, which is, because of the relative momentum, expected at $am \approx 2 \cdot 0.27 + \frac{\pi}{L}$. Of course this is a crude estimate and higher state contamination is present because of the few usable time steps. The operators used therefore have too little overlap with this state or any other lower lying state. The volume dependency of the effective mass is shown in Figure 7. It is, as expected, quite small.

Figure 5: The effective masses for parameter set 1 and $N = 12$ at different smearing levels.

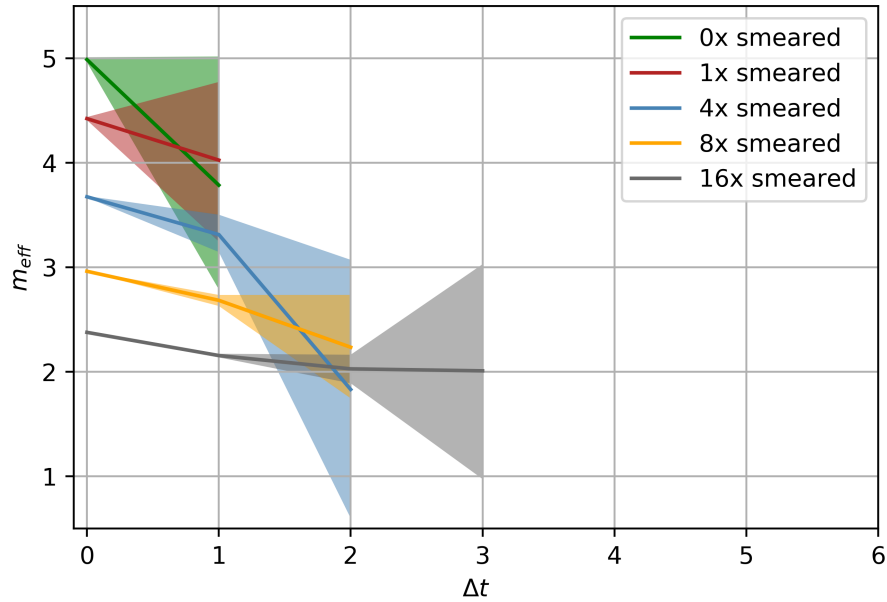


Figure 6: The effective masses for parameter set 1 and $N = 16$ at different smearing levels.

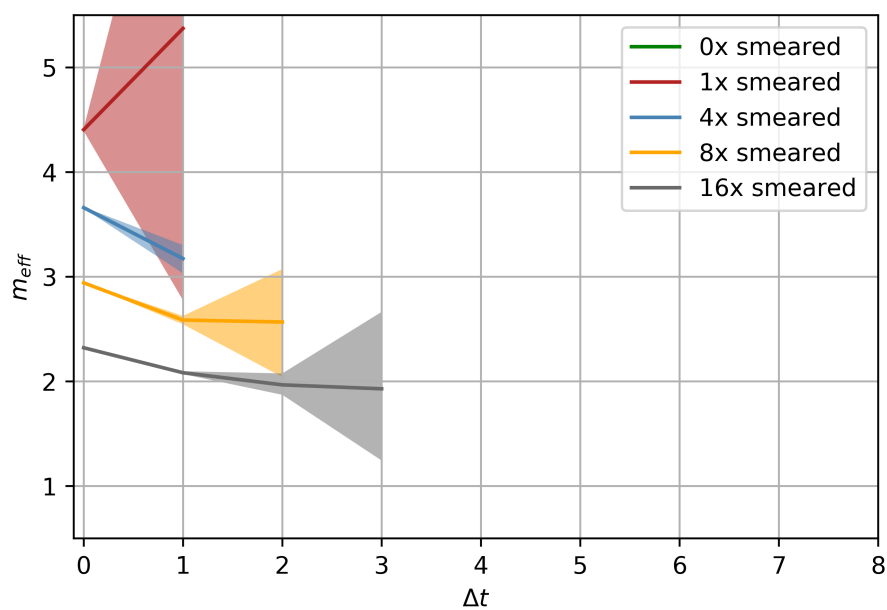
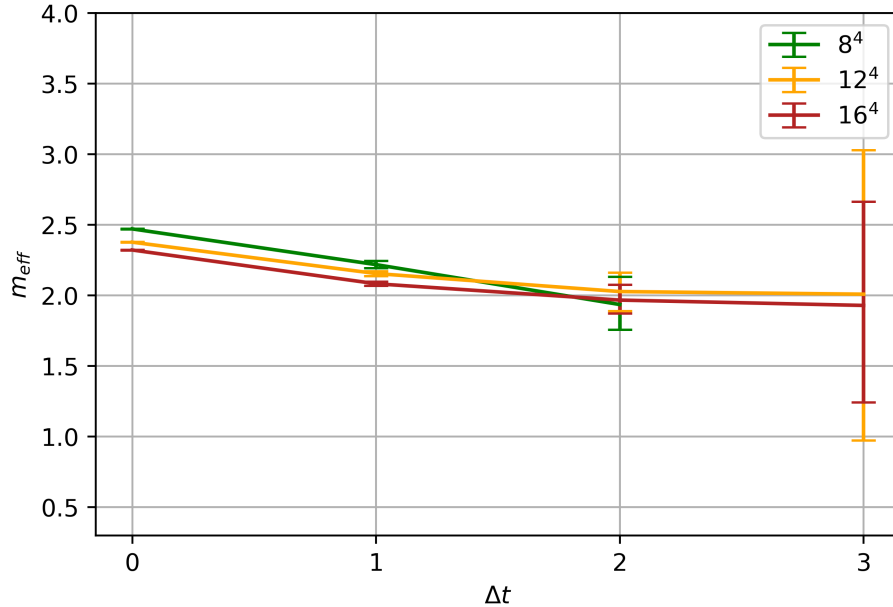


Figure 7: The effective masses for parameter set 1 and $N = 8, 12, 16$ after 16 smearing steps.



5.2 Parameter set 2

The parameters for the second set of calculations are $\beta = 5.082$, $\kappa = 0.249$ and $\lambda = 0.7$. At this phase space point the lattice spacing is $a^{-1} = 636\text{GeV}$, the coupling is $\alpha_{200\text{GeV}} = 0.170$ and the mass ratio is $m_{1_3^-}/m_{0_1^+} = 80\text{GeV}/123(19)\text{GeV}$. All errors are $< 1\%$, except when specified otherwise. The masses in the plots are again given in lattice units.

Figure 8 and 9 show the correlator and the effective mass for lattice size $N = 8$ for different smearing levels, respectively. The operators don't show qualitatively different behaviour at this phase space point, compared to the one of parameter set 1.

Figure 8: The correlators for parameter set 2 for lattice size $N = 8$ for different smearing levels

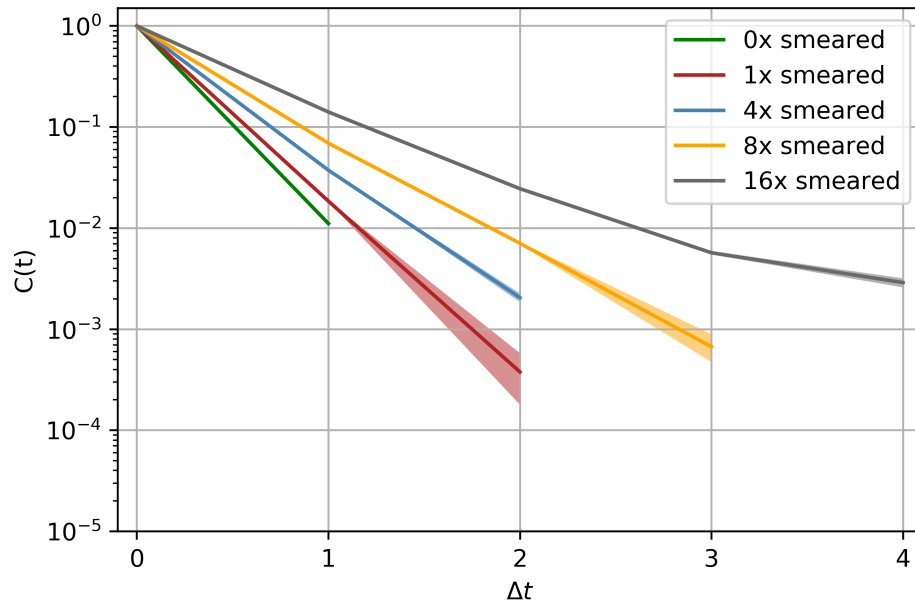
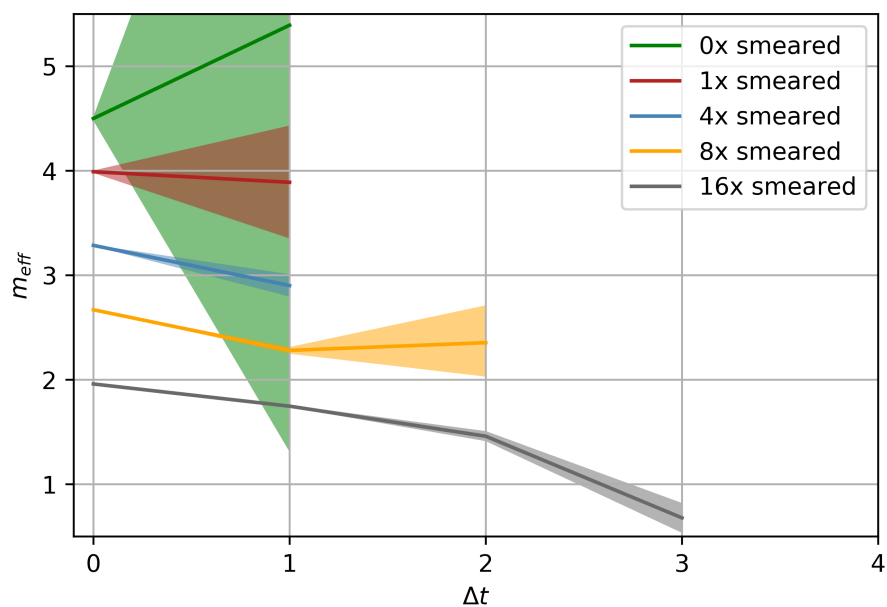


Figure 9: The effective mass for parameter set 2 for lattice size $N = 8$ and different smearing levels.



6 Conclusion

In this thesis we discussed a $SU(2)$ -Yang-Mills-Higgs theory and determined the effective masses of three 1_1^- -operators. These operators, introduced in Section 2.6, were determined at three lattice sizes, $N = 8, 12, 16$, at different smearing steps, i.e. 0, 1, 4, 8, 16, and using 957000 configurations. These results for the two parameter sets are displayed in Chapter 5. These plots show that the operators have too little overlap with hypothetical low mass states. Such a low mass state could have been associated with a Z' -like particle. A scattering state with the mass of two Higgs bosons and relative momentum was not detected either. Furthermore it was shown that the operators are very noisy, and large statistics and many smearing steps are needed to get significant results. The intent of this thesis, finding a Z' -like state, i.e. a scalar singlet vector state with a low mass, was thus not achieved. Since no such state was found, the results do not disagree with standard perturbation theory and/or GIPT. Further progress in this regard could be made by devising new operators with the same quantum numbers or creating an operator basis and performing a variational analysis with a large set of measurements.

7 Appendix - Wilson loop implementation

The following source code is the implementation of equation (7). Most of the code is dedicated to finding the proper spatial argument for the links. The Wilson loop operator needs to constitute a continuous path through space, see Figure 1. Because for different values of the indices μ, ν and ρ in $W_{\mu\nu\rho}$ the operator points in different directions in space, the spatial arguments of the links have to change.

- `x` is the time coordinate.
- `muIn` is the value of the index μ in $W_{\mu\nu\rho}$.
- `su2` is a custom class for `su2` matrices.

```
long double W(int muIn, int nuIn, int rhoIn, int x/*time*/){

    int inputIndex[4]={0,muIn,nuIn,rhoIn};

    su2 U[8];
    // Contains the 8 links
    // 0    1    2    3          4    5          6          7
    // U_mu U_mu U_nu U_mu^\dag U_rho U_mu^\dag U_rho^\dag U_nu^\dag

    int index[8]={1,1,2,-1,3,-1,-3,-2};
    // Contains the direction of the 8 links.
    // mu -> 1, -mu -> -1
    // nu -> 2, -nu -> -2
    // rho-> 3, -rho-> -3

    bool step[8];
    // Tells you whether you have taken the i-th step through space

    vec vx;
    vx.x=x;
    su2 sum=kZeroSU2;
```

- `vx` is the vector that specifies the lattice point.
- `kZeroSU2` is the the 2×2 0-matrix.
- `vx.t` contains the physical `x` coordinate.
- `vx.z` contains the physical `y` coordinate.

- vx.y contains the physical z coordinate.
- Now follows a loop over the three space dimensions.

```

for(vx.t=0;vx.t<kNt;++vx.t) {
  for(vx.z=0;vx.z<kNz;++vx.z) {
    for(vx.y=0;vx.y<kNy;++vx.y) {
      vec arg=vx;
      for(int i=0; i<8; ++i)
        step[i]=false;

      for(int i=0; i<8; ++i) {
        int currentDirection = abs(inputIndex[abs(index[i ])]);
        int lastDirection;
        if(i>0)
          lastDirection = abs(inputIndex[abs(index[i-1])]);
        bool negativeDirection=( index[i]*inputIndex[abs(index[i])] < 0 );

        // If last step has not been taken yet and i>0: Take step
        if( (step[i-1]==false) && (i>0) ){
          arg=vaddP(arg,e[lastDirection],currentDirection);
          step[i-1]=true;
        }

        // If U is "daggered": Take current step
        if( negativeDirection ){
          arg=vaddP(arg,ne[currentDirection],currentDirection);
          step[i]=true;
        }
        arg.mu=currentDirection;

        // Give U[i] the link values
        if( negativeDirection )
          U[i]=minv(vmap(arg,fGFLattice));
        else
          U[i]=vmap(arg,fGFLattice);
      }
      sum=sum+(U[0]*U[1]*U[2]*U[3]*U[4]*U[5]*U[6]*U[7]);
    }
  }
}

```

```
    }  
    return mtrace(sum).real()/2.L;  
}
```

- `vaddP` is a function, that adds vectors respecting the periodic boundary conditions of the lattice.
- `e[i]` is a vector that points in the positive i -direction.
- `ne[i]` is a vector that points in the negative i -direction.
- `vmap(vector, field)` is a function that returns the field value (here a su_2 -matrix) at the lattice point specified by the vector.

References

- [1] David J Griffiths. *Introduction to elementary particles; 2nd rev. version*. Physics textbook. Wiley, New York, NY, 2008.
- [2] J. Fröhlich, G. Morchio, and F. Strocchi. *Phys. Lett.*, 97B:249–252, 1980.
- [3] J. Fröhlich, G. Morchio, and F. Strocchi. *Nucl. Phys.*, B190:553–582, 1981.
- [4] Axel Maas. *Eur. Phys. J.*, C71:1548, 2011.
- [5] Axel Maas. *Mod. Phys. Lett.*, A28:1350103, 2013.
- [6] Axel Maas and Tajdar Mufti. *JHEP*, 04:006, 2014.
- [7] Michael E. Peskin and Daniel V. Schroeder. *An Introduction to quantum field theory*. Addison-Wesley, Reading, USA, 1995.
- [8] Chen-Ning Yang and Robert L. Mills. *Phys. Rev.*, 96:191–195, 1954.
- [9] Axel Maas. *arXiv:1712.04721*, 2017.
- [10] Axel Maas and Tajdar Mufti. *PoS, LATTICE 2014*:060, 2014.
- [11] Francesco Knechtli and Rainer Sommer. *Phys. Lett.*, B440:345–352, 1998.
- [12] H. G. Evertz, J. Jersak, C. B. Lang, and T. Neuhaus. *Phys. Lett.*, B171:271–279, 1986.
- [13] Eduardo H. Fradkin and Stephen H. Shenker. *Phys. Rev.*, D19:3682–3697, 1979.
- [14] C. B. Lang, C. Rebbi, and M. Virasoro. *Phys. Lett.*, 104B:294, 1981.
- [15] Axel Maas and Tajdar Mufti. *Phys. Rev.*, D91(11):113011, 2015.
- [16] Mark Wurtz and Randy Lewis. *Phys. Rev.*, D88:054510, 2013.
- [17] B Berg and A Billoire. *Nuclear Physics B*, 221:109–140, 07 1983.
- [18] A. Abulencia et al. *Phys. Rev. Lett.*, 96:211801, 2006.
- [19] I. Montvay and G. Munster. *Quantum fields on a lattice*. Cambridge University Press, 1997.
- [20] O. Philipsen, M. Teper, and H. Wittig. *Nucl. Phys.*, B469:445–472, 1996.
- [21] Thomas A. DeGrand, Anna Hasenfratz, and Tamas G. Kovacs. *Nucl. Phys.*, B520:301–322, 1998.

Acknowledgements

This thesis would not have been possible without the support of my colleagues and family. First, I want to thank my supervisor Axel Maas, for helping me at every step of this thesis with many enlightening conversations and good advice. Furthermore I want to thank Sebastian Raubitzek, Pascal Törek and Vincenzo Afferrante for helpful tips and just for being great colleagues. Christian Rohrhofer, Ursula Winkler and Fanny Maetz helped me a lot tackling technical and administrative problems. Thank you for that.

Furthermore I want to thank my employer, Virtual Vehicle, for the possibility to work, while finishing this thesis.

And last but certainly not least, I want to thank my wife for taking a load off my back when i needed it, for keeping me going when I slowed down and for being the best partner one can wish for. I want to thank my son and my daughter for keeping me sane during this stressful time and for taking my mind off work and I want to thank my family for all the support during my entire time at university.